GEOLOGY | THE GEOLOGICAL SOCIETY OF AMERICA®

https://doi.org/10.1130/G48967.1

Manuscript received 18 February 2021
Revised manuscript received 27 April 2021
Manuscript accepted 10 May 2021

Published online 12 July 2021



# Construction of the Lesser Himalayan–Subhimalayan thrust belt: The primary driver of thickening, exhumation, and high elevations in the Himalayan orogen since the middle Miocene

Sean P. Long[1] and Delores M. Robinson[2]
[1]School of the Environment, Washington State University, Pullman, Washington 99164, USA
[2]Department of Geological Sciences, University of Alabama, Tuscaloosa, Alabama 35487, USA

## ABSTRACT

**Documenting the structural evolution of the Himalayan orogen is fundamental for understanding the dynamics of collisional orogenesis. We argue that the importance of deformation in the frontal, Lesser Himalayan–Subhimalayan (LH-SH) portion of the Himalayan thrust belt for driving crustal thickening over the past ~15–13 m.y. has long been overlooked. To quantify its contribution to thickening, we measured parameters from 22 published cross sections that span the length of the orogen. The mean structural uplift accomplished by the LH-SH thrust belt increases from 10–15 km in the eastern half of the orogen to 15–23 km in the western half. An antiformal culmination constructed by LH duplexing is observed across the orogen and increases in structural height (to as much as 15–20 km) and north-south width moving westward. Construction of the culmination was the primary mechanism for building and maintaining wedge taper. The westward scaling of culmination size is accompanied by doubling and tripling of LH-SH shortening and accretion magnitude, respectively; when combined with a consistent orogen-wide modern taper angle (11° ± 2°), this indicates that duplexing facilitated the growth of an overall larger orogenic wedge moving westward. Following the initial southward propagation of deformation into LH rocks at ca. 15–13 Ma, the Himalayan orogenic wedge has been characterized by stacking of multiple thin, small-displacement thrust sheets to develop a high-taper orogenic wedge. Thus, LH-SH deformation has had a profound effect on driving thickening, exhumation, and the attainment of high elevations since the middle Miocene.**

## INTRODUCTION

Collisional orogens can strongly impact climate, biologic diversity, and society (e.g., seismic and landslide hazards, natural resources, and water availability). Therefore, understanding how these dynamic orogenic systems evolve is an imperative grand challenge for continental tectonics. In the Himalayan-Tibetan orogen, which is commonly viewed as a modern archetype through which we can understand Earth's older collisional orogens, the deformation processes that have constructed our highest continental mountain range have been debated considerably (e.g., Kohn, 2008). Over the past 20 years, most research on Himalayan structural geology has focused on the ca. 25–15 Ma emplacement of mid-crustal metamorphic rocks of the Greater Himalayan (GH) package (e.g., Beaumont et al., 2001; Law et al., 2006; Cottle et al., 2015). Consequently, we argue that the important contribution of younger (ca. 15–0 Ma) deformation in the frontal part of the orogen, consisting of at least ~200–400 km of shortening accommodated in the Lesser Himalayan–Subhimalayan (LH-SH) portion of the thrust belt (e.g., Bhattacharyya and Ahmed, 2016), has been comparatively overlooked. The purpose of this study is to quantify the profound influence of the LH-SH thrust belt on Himalayan crustal thickening by measuring parameters including structural elevation and accreted area from 22 published cross sections that span a 2200 km arc-parallel distance. We emphasize that shortening in the LH-SH thrust belt was the primary driver for construction of a high-taper orogenic wedge over the past ~15–13 m.y. and was therefore of first-order importance for generating Earth's highest-elevation mountain range.

## TECTONIC FRAMEWORK

### Himalayan-Tibetan Orogen

The Himalayan-Tibetan orogen is the product of Cenozoic convergence between India and Asia (e.g., Yin, 2006). The Himalayan thrust belt comprises the southern portion of the orogen, lying between the Indus-Yarlung suture zone and the Main Frontal thrust (MFT) (Fig. 1) and, from north to south, is divided into: (1) the Tethyan Himalayan package of sedimentary rocks, which overlies GH rocks across the top-down-to-the-north South Tibetan detachment system (STDS); (2) the GH package of amphibolite- to granulite-facies metasedimentary and igneous rocks, which was buried to ~30–40 km depths prior to its south-directed translation above the Main Central thrust (MCT) between ca. 25 and 15 Ma (e.g., Cottle et al., 2015); (3) the LH package of Paleoproterozoic–Paleogene, dominantly greenschist-facies metasedimentary rocks, which has been deformed into a south-directed thrust belt; and (4) the SH package of Neogene synorogenic sedimentary rocks, which is carried in frontal thrust sheets.

### Lesser Himalayan–Subhimalayan Thrust Belt

Along the length of the orogen, 3–5 km of Paleoproterozoic (ca. 1.9–1.75 Ga) quartzite and phyllite account for the largest volume of LH rocks (Fig. 2; e.g., Yin, 2006). In Arunachal Pradesh (India), Bhutan, and Sikkim (India), Paleoproterozoic LH rocks are overlain by 2–5 km of Neoproterozoic–Ordovician quartzite, phyllite, and marble and Permian diamictite and sandstone (Figs. 2A–2C; e.g., Long et al., 2011). In Nepal, the LH section consists of 5–8 km of Paleo- and Mesoproterozoic quartzite, phyllite, and marble and <1 km of Mesozoic–Paleogene sandstone and

CITATION: Long, S.P., and Robinson, D.M., 2021, Construction of the Lesser Himalayan–Subhimalayan thrust belt: The primary driver of thickening, exhumation, and high elevations in the Himalayan orogen since the middle Miocene: Geology, v. 49, p. 1283–1288, https://doi.org/10.1130/G48967.1

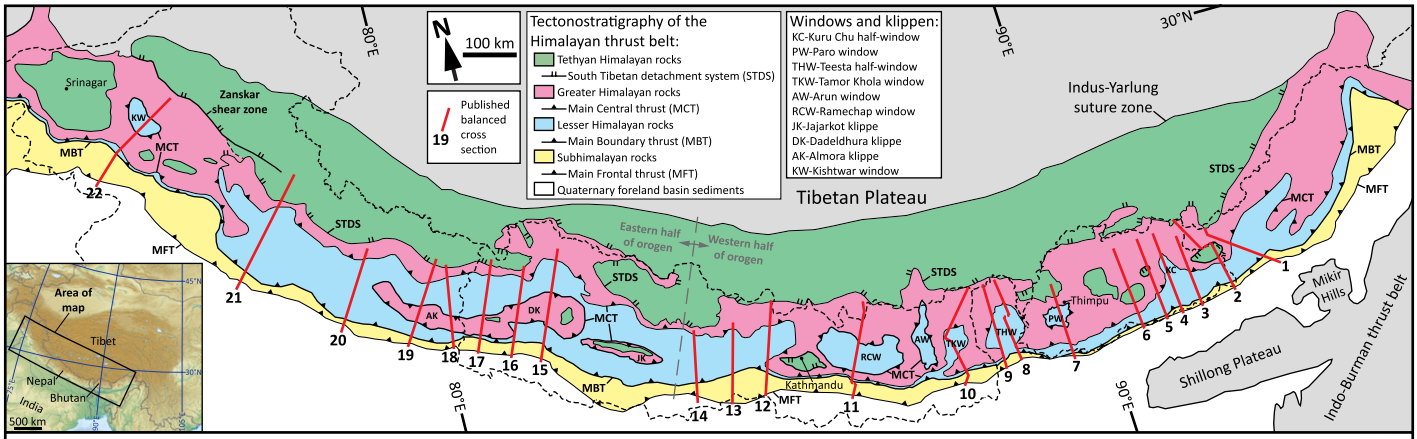


**Published cross sections (east to west):**

1-Western Arunachal Pradesh (DeCelles et al., 2016)
2-Sakteng, eastern Bhutan (McQuarrie et al., 2019)
3-Trashigang, eastern Bhutan (Long et al., 2011)
4-Kuru Chu, eastern Bhutan (Long et al., 2011)
5-Bumthang Chu, central Bhutan (Long et al., 2011)
6-Mangde Chu, central Bhutan (Long et al., 2011)
7-Wang Chu, western Bhutan (McQuarrie et al., 2014)
8-Eastern Sikkim (Parui and Bhattacharyya, 2018)
9-Western Sikkim (Bhattacharyya et al., 2015)
10-Tamor Khola, western Nepal (Schelling and Arita, 1991)
11-Ramechap, western Nepal (Schelling, 1992)
12-Budhi Gandaki, central Nepal (Khanal and Robinson, 2013)
13-Marsyangdi, central Nepal (Khanal, 2014)
14-Kaligandaki, central Nepal (Robinson and Martin, 2014)
15-Simikot, western Nepal (Robinson et al., 2006)
16-Chainpur, western Nepal (Robinson et al., 2006)
17-Api, western Nepal (Robinson et al., 2006)
18-Eastern Kamaon (Mandal et al., 2019)
19-Almora, Kumaon and Garwhal (Srivastava and Mitra, 1994)
20-Deoprayag, Kumaon and Garwhal (Srivastava and Mitra, 1994)
21-Himachal Pradesh (Webb, 2013)
22-Eastern Kashmir (Gavillot et al., 2018)

**Figure 1. Simplified geologic map of the Himalayan thrust belt (modified from Long et al., 2011; Webb, 2013; Gavillot et al., 2018; Mandal et al., 2019), showing locations of compiled cross sections.**

shale (Figs. 2D and 2E; e.g., Robinson et al., 2006). In northwestern India, Paleoproterozoic LH rocks are overlain by 3–5 km of Neoproterozoic–Cambrian sandstone, shale, and limestone and <1 km of Cretaceous–Paleogene limestone and sandstone (Figs. 2F–2H; e.g., Webb, 2013). At the southern edge of the orogen, 5–7 km of Neogene conglomerate, sandstone, and shale of the SH Siwalik Group restore stratigraphically above LH rocks (Fig. 2).

The LH-SH thrust belt, which consists of all thrust sheets between the MCT and the MFT, exhibits a similar first-order structural architecture along the length of the orogen, consisting of (1) a hinterland duplex and associated antiformal culmination, and (2) a frontal imbricate zone (Fig. 2A). The duplex consists of repeated horses of LH rocks, which structurally elevated and folded overlying GH rocks. In Bhutan, the MCT acted as the roof thrust for Paleoproterozoic horses in a northern duplex, and the Shumar thrust acted as the roof thrust for Neoproterozoic–Paleozoic horses in a southern duplex (Fig. 2B; Long et al., 2011). In Sikkim, Paleoproterozoic horses feed slip into the Pelling thrust ~4 km below the MCT, and underlying Paleoproterozoic–Paleozoic horses feed slip into the Ramgarh thrust; these two duplex systems are stacked on top of each other (Fig. 2C; e.g., Bhattacharyya et al., 2015). In central Nepal, the Ramgarh-Munsiari thrust carries a 1–3-km-thick sheet of Paleoproterozoic rocks below the MCT, while the structurally lower Trishuli thrust acted as the roof thrust for underlying horses (Fig. 2D; Khanal and Robinson, 2013). In western Nepal and northwestern India, the Ramgarh-Munsiari thrust carries a 2–5-km-thick sheet of Paleoproterozoic rocks beneath the MCT and acted as the roof thrust for duplexing (Figs. 2E and 2F; Robinson et al., 2006), and the underlying Tons thrust acted as a second roof thrust farther to the northwest in India (Fig. 2G; Webb, 2013).

An important consequence of LH duplexing is the generation of an antiformal culmination, which passively uplifted and folded the MCT and overlying GH rocks (e.g., Robinson et al., 2003). In Arunachal Pradesh and Bhutan, the culmination is defined by an east-trending antiform mapped within GH rocks, with local erosional windows into LH rocks (Figs. 1 and 2A; e.g., Long et al., 2011). From Sikkim westward, the significant structural height of the culmination has generated large regions of exposed LH rocks, with synformal foreland klippen of GH rocks preserved in several places (Figs. 1, 2C–2H; e.g., Robinson et al., 2006).

The frontal imbricate zone of the LH-SH thrust belt consists of north-dipping thrust sheets that carry progressively younger LH units toward the south and thrust sheets of SH rocks near the MFT (Fig. 2). The deformation geometry of SH rocks varies from a single thrust sheet in Bhutan and Sikkim (Figs. 2A–2C) to multiple thrust sheets in the rest of the orogen (Figs. 2D–2H).

## CROSS-SECTION PARAMETERS

We measured the following parameters from 22 published balanced cross sections, which are distributed across a 2200 km arc-parallel distance (Fig. 1). Using the MFT trace as a reference point, at a distance of every 2 km along each section line we measured (see Fig. 2 inset; also see the Supplemental Material[1] for supporting data): (1) the surface elevation; (2) the depth to the basal décollement; (3) the total structural elevation accomplished by the LH-SH thrust belt (black arrows in Fig. 2 inset), measured by comparing the elevation of the structurally highest LH or SH stratigraphic contact above or below the modern surface to its elevation at or beneath the basal décollement; and (4) the preserved structural elevation accomplished by the LH-SH thrust belt (gray arrows), measured by comparing the elevation of the stratigraphic level exposed at the modern surface to its elevation at or beneath the basal décollement. We also measured: (5) the total accreted area of LH-SH rocks (green line in Fig. 2 inset), measured relative to the structurally highest LH or SH rocks shown above the modern surface; (6) the preserved accreted area of LH-SH rocks (orange line), measured relative to the modern surface; (7) the southern and northern extents, peak height, and elevated area of the LH duplex culmination, using the basal elevation of the MCT in the frontal limb as a reference height (blue line); and (8) the complete or minimum preserved structural thickness of GH rocks in foreland and hinterland positions (pink arrows). We also compiled published estimates of the minimum shortening accomplished by the LH-SH thrust belt on

[1]Supplemental Material. Supplemental figures and tables that provide supporting data for the compiled cross sections and the measured parameters, as well as text that summarizes the tectonostratigraphic units on each cross section. Please visit https://doi.org/10.1130/GEOL.S.14781936 to access the supplemental material, and contact editing@geosociety.org with any questions.

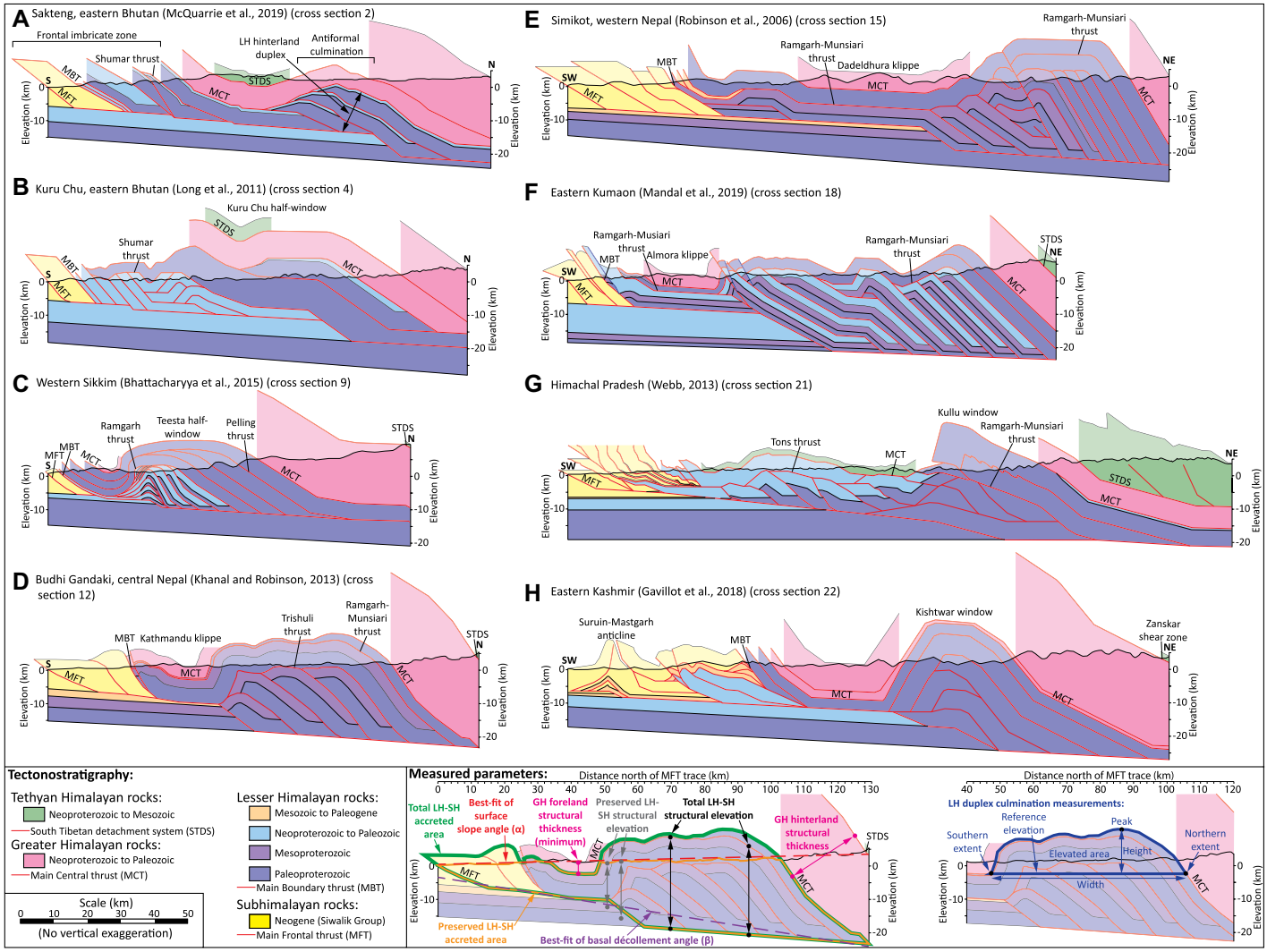


**Figure 2. Representative cross sections of the Lesser Himalayan–Subhimalayan (LH-SH) thrust belt, ordered from east to west (cross section numbers referenced to Figure 1; all 22 cross sections are shown in the Supplemental Material [see footnote 1]). Inset diagrams on lower right illustrate parameters measured from cross sections.**

each cross section (see the supporting data in the Supplemental Material).

## RESULTS

Using best-fit lines of the elevation and depth to basal décollement measurements, we calculated the surface slope ($\alpha$), basal slope ($\beta$), and taper angles ($\alpha + \beta$) for each cross section (Fig. 3A). $\alpha$ angles are typically between 1° and 2° (average of 1.6° ± 0.6°; all errors are reported at 1$\sigma$). $\beta$ angles are typically between 7° and 10° but are as high as 12°–13° in eastern and central Nepal (orogen-wide average of 9.2° ± 1.8°). Taper varies from ~8.5°–10° from Arunachal Pradesh to eastern Sikkim, to ~13°–15° from western Sikkim to central Nepal, to ~9°–12° in the western half of the orogen, with an orogen-wide average of 10.8° ± 2.1°.

Minimum LH-SH shortening increases from ~180–300 km in the eastern half of the orogen to ~350–400 km in the western half (Fig. 3B). Percent shortening generally increases westward, from ~55%–70% to ~65%–75% (Fig. 3C). The accreted area of LH-SH rocks increases westward (Fig. 3D), with total area increasing from ~700–1700 km$^2$ to ~1800–3000 km$^2$ and preserved area increasing from ~600–1600 km$^2$ to ~1500–2300 km$^2$.

The LH duplex culmination is typically located between ~30 and 120 km north of the MFT but is locally as much as ~100–170 km north of the MFT in the western half of the orogen (Fig. 3E). The average north-south width of the culmination increases from 44 ± 16 km in the eastern half of the orogen to 66 ± 15 km in the western half (Fig. 3E). The height and elevated area of the culmination increase (albeit nonlinearly) westward from ~4–10 km to ~8–22 km and from ~50–300 km$^2$ to ~300–700 km$^2$, respectively (Figs. 3F and 3G).

The structural thickness of hinterland exposures of GH rocks (both complete and minimum) generally varies from 15 to 31 km between Arunachal Pradesh and central Nepal (cross sections 1–12), which decreases westward to 6–12 km with the exception of a 25-km-thick section in Kashmir (Fig. 3H). Complete and minimum thicknesses of foreland GH exposures are typically 4–8 km.

In the eastern half of the orogen, the mean total structural elevation accomplished by the LH-SH thrust belt, which represents a proxy for cumulative rock uplift, increases from ~5 to ~15 km between 0 and 50 km north of the MFT, stays constant at ~15 km between 50 and 80 km, and decreases from ~15 to ~3 km between 80 and 130 km north of the MFT (Fig. 4A). In the western half of the orogen, this parameter increases from ~5 to ~20 km between 0 and 55 km north of the MFT, stays constant at ~20–23 km between 55 and 135 km, and decreases from ~20 to ~13 km between 135 and 160 km north of the MFT.

In the eastern half of the orogen, the mean preserved structural elevation, which represents a proxy for the net vertical thickening accomplished

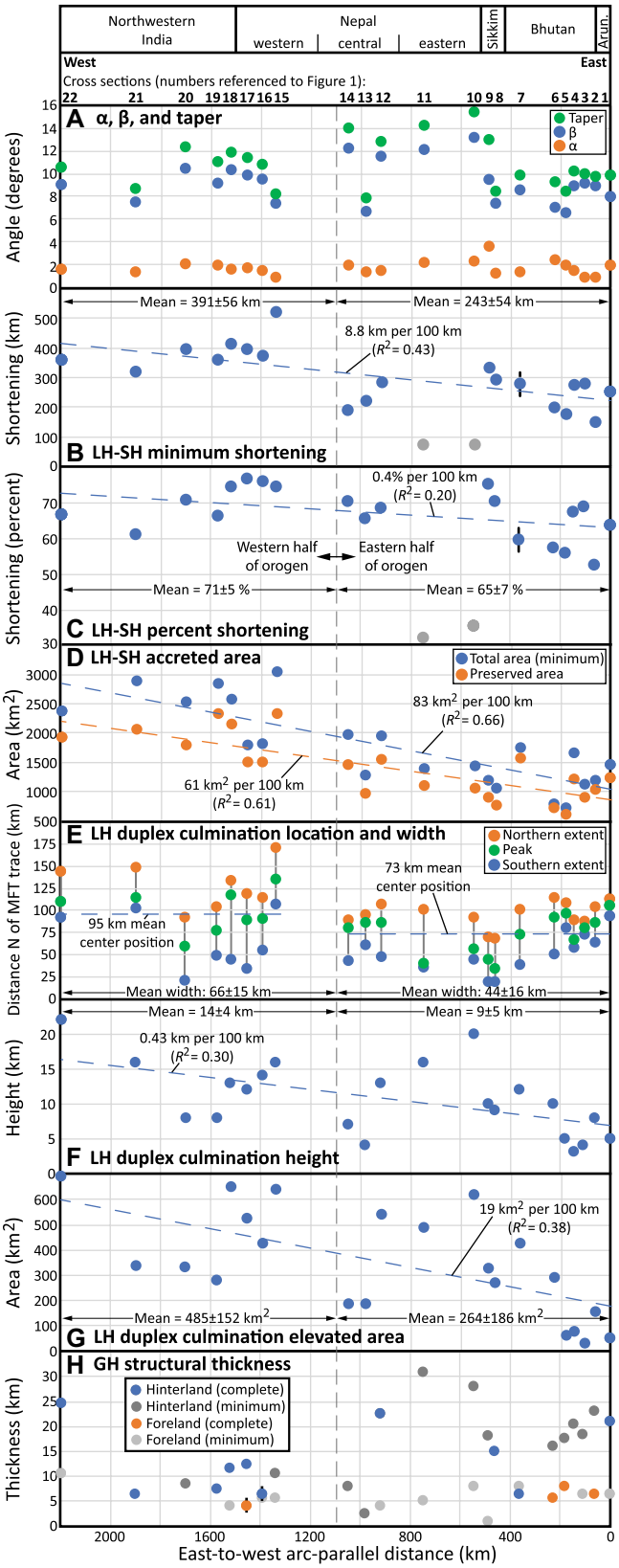


**Figure 3. Graphs of Lesser Himalayan–Subhimalayan (LH-SH) cross section parameters versus arc-parallel distance (see Fig. 2 for parameter definitions) (taper = α + β). For B and C, estimates of Schelling and Arita (1991) and Schelling (1992) (shown in gray) are considered outliers because they do not account for intra-LH structures (e.g., Long et al., 2011). For B, C, and H, data points that have a range of values are shown with error bars. Arun.—Arunachal Pradesh; GH—Greater Himalayan.**

by the LH-SH thrust belt, increases from ~3 to ~13 km between 0 and 50 km north of the MFT, stays constant at ~13 km between 50 and 85 km, and decreases from ~13 to ~3 km between 85 and 125 km north of the MFT (Fig. 4B). In the western half, this parameter increases from ~5 to ~13 km between 0 and 20 km north of the MFT, increases from ~13 to ~20 km between 20 and 105 km, and decreases from ~20 to ~10 km between 105 and 160 km north of the MFT.

## DISCUSSION

Duplex culminations similar to those observed in the LH-SH thrust belt have been produced in analogue models of thrust belts and are attributed to sustained basal accretion, which drives localized surface uplift and enhances erosion, eventually resulting in unroofing of the accreted rocks and isolation of structurally overlying rocks in a synformal foreland klippe (e.g., Perrin et al., 2013). Duplexing is a common process by which the hinterland portions of thrust belts sustain the taper angle necessary for continued forward propagation (e.g., Dahlen, 1990; DeCelles and Mitra, 1995). The persistence of the LH duplex culmination along the length of the orogen suggests that duplexing was the primary mechanism for building and maintaining taper over the duration of deformation in the LH-SH thrust belt. The initiation of LH deformation represents an important transition from long-distance translation of the thick GH package to the style of a foreland thrust belt dominated by critical taper dynamics, characterized by stacking of multiple thin, short, small-displacement LH thrust sheets to build a high-taper orogenic wedge (e.g., DeCelles et al., 2016). Thermochronometry, thermo-kinematic modeling, and dated field relationships bracket the timing of initial LH deformation, most commonly dating the emplacement of the LH thrust sheet immediately beneath the MCT, across a narrow time interval of ca. 15–13 Ma (though a few estimates range as old as ca. 17 Ma and as young as ca. 11 Ma), with no obvious timing trend along strike (e.g., Kohn et al., 2004; Robinson et al., 2006; Célérier et al., 2009; Webb, 2013; McQuarrie et al., 2014, 2019; Bhattacharyya et al., 2015; DeCelles et al., 2016; Colleps et al., 2018; Gavillot et al., 2018; Ghoshal et al., 2020). This followed, and perhaps partially overlapped with, a period of major normal-sense shearing on the overlying STDS along much of the orogen between ca. 25 and ca. 13 Ma (e.g., Kellett et al., 2018) and roughly coincides with the ca. 12 Ma intensification of the Indian monsoon (e.g., Dettman et al., 2003). Therefore, the initiation of LH duplexing may represent a response to restoration of the taper lost to displacement on the STDS and/or to monsoon-induced erosion, and was likely facilitated by migration of the deformation front from the stronger, largely meta-igneous GH package into weaker, micaceous LH sedimentary rocks, which required duplexing to maintain the taper necessary to drive forward propagation (e.g., DeCelles and Mitra, 1995).

The north-south cross-sectional length of the LH-SH thrust belt, magnitude of LH-SH shortening, accretion, and structural elevation, and dimensions of the LH duplex culmination all increase westward along the orogen (Figs. 2–4). When combined with the broadly consistent orogen-wide modern taper angle (11° ± 2° average), this indicates that construction of a

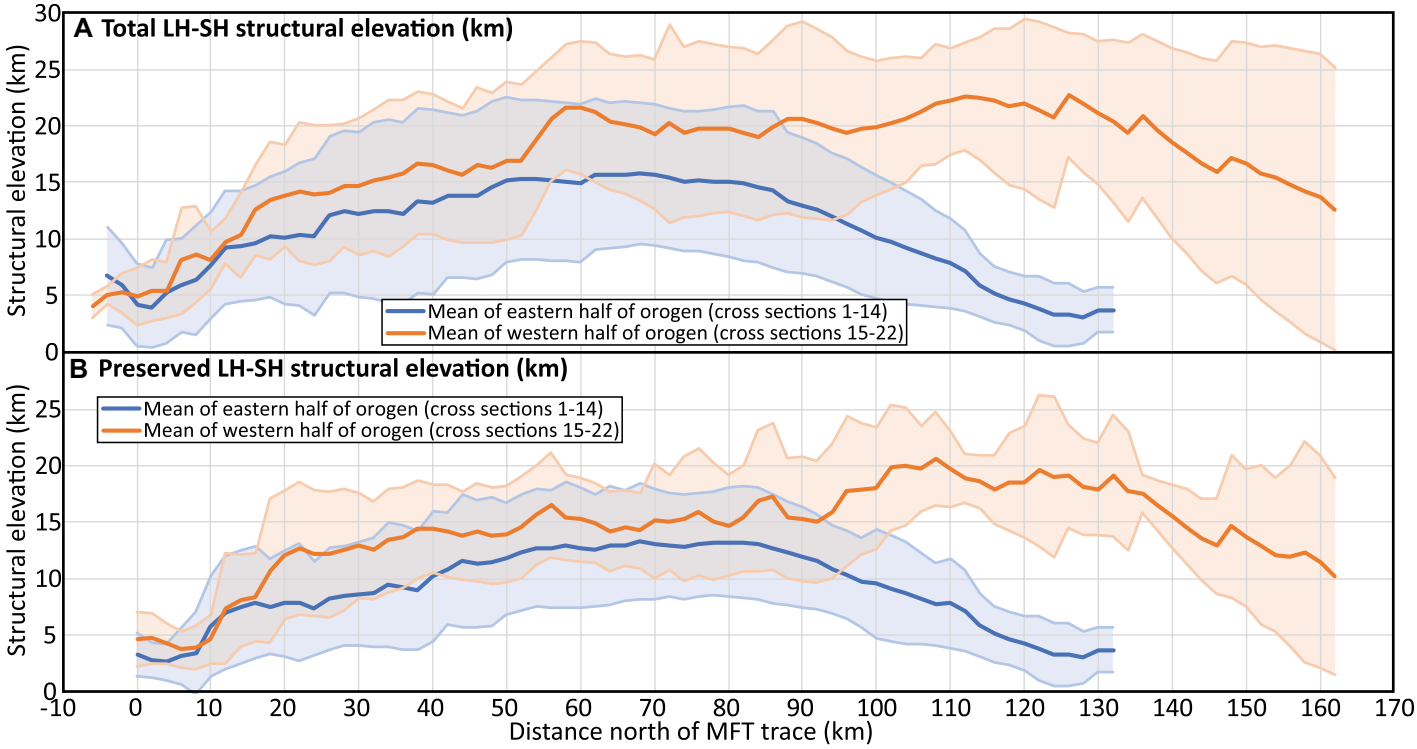


**Figure 4. Graphs of mean structural elevation accommodated by the Lesser Himalayan–Subhimalayan (LH-SH) thrust belt. Error envelopes are ±1σ.**

taller and wider duplex was required to allow for the sustained growth of an overall larger orogenic wedge moving westward. This could be the consequence of one or more factors, including

(1) A greater original north-south width of LH basins moving westward, and thus a larger volume of LH rocks available for accretion (e.g., Bhattacharyya and Ahmed, 2016).

(2) Along-strike variation in convergence partitioning between the LH-SH thrust belt and the Tibetan Plateau. Long-term India-Asia convergence rates decrease 20% between the eastern (~5 cm/yr from 15 to 0 Ma) and western syntaxes (~4 cm/yr from 20 to 0 Ma) (van Hinsbergen et al., 2011). Thus, LH-SH shortening over the past ~15–13 m.y. can account for ~30%–45% of India-Asia convergence in the east and ~70%–80% in the west.

(3) Erosionally limited outward growth of the LH-SH thrust belt as a result of eastward-increasing monsoon precipitation (e.g., Hirschmiller et al., 2014). While climatic controls cannot be ruled out, this scenario is not favored by the eastward decrease in LH-SH percent shortening (e.g., McQuarrie et al., 2008).

Regardless of the origin of the westward increase in shortening, accretion, and duplex dimensions, the net vertical thickening accomplished by the LH-SH thrust belt (~10–13 km in the east and ~15–20 km in the west) illustrates that LH duplexing was a first-order thickening mechanism, which outweighed the contribution of emplacement of the ~6–12-km-thick GH package in the western half of the orogen. The transition to duplexing-dominated LH deformation was of primary importance for construction of the high-taper orogenic wedge (and thus the high elevations) observed today and has been the primary driver of uplift-related exhumation over the past ~15–13 m.y.


## ACKNOWLEDGMENTS

This paper was inspired by the work of many outstanding Himalayan geologists, including P. DeCelles and N. McQuarrie. We thank K. Bhattacharyya, A. Laskowski, C. Parui, and M. Taylor for thoughtful reviews.


## REFERENCES CITED


Beaumont, C., Jamieson, R.A., Nguyen, M.H., and Lee, B., 2001, Himalayan tectonics explained by extrusion of a low-viscosity crustal channel coupled to focused surface denudation: Nature, v. 414, p. 738–742, https://doi.org/10.1038/414738a.

Bhattacharyya, K., and Ahmed, F., 2016, Role of initial basin width in partitioning total shortening in the Lesser Himalayan fold-thrust belt: Insights from regional balanced cross-sections: Journal of Asian Earth Sciences, v. 116, p. 122–131, https://doi.org/10.1016/j.jseaes.2015.11.012.

Bhattacharyya, K., Mitra, G., and Kwon, S., 2015, Geometry and kinematics of the Darjeeling–Sikkim Himalaya, India: Implications for the evolution of the Himalayan fold-thrust belt: Journal of Asian Earth Sciences, v. 113, p. 778–796, https://doi.org/10.1016/j.jseaes.2015.09.008.

Célérier, J., Harrison, T.M., Beyssac, O., Herman, F., Dunlap, W.J., and Webb, A.A.G., 2009, The Kumaun and Garwhal Lesser Himalaya, India: Part 2. Thermal and deformation histories: Geological Society of America Bulletin, v. 121, p. 1281–1297, https://doi.org/10.1130/B26343.1.

Colleps, C.L., McKenzie, N.R., Stockli, D.F., Hughes, N.C., Singh, B.P., Webb, A.A.G., Myrow, P.M., Planavsky, N.J., and Horton, B.K., 2018, Zircon (U-Th)/He thermochronometric constraints on Himalayan thrust belt exhumation, bedrock weathering, and Cenozoic seawater chemistry: Geochemistry Geophysics Geosystems, v. 19, p. 257–271, https://doi.org/10.1002/2017GC007191.

Cottle, J.M., Larson, K.P., and Kellett, D.A., 2015, How does the mid-crust accommodate deformation in large, hot collisional orogens? A review of recent research in the Himalayan orogen: Journal of Structural Geology, v. 78, p. 119–133, https://doi.org/10.1016/j.jsg.2015.06.008.

Dahlen, F.A., 1990, Critical taper model of fold-and-thrust belts and accretionary wedges: Annual Review of Earth and Planetary Sciences, v. 18, p. 55–99, https://doi.org/10.1146/annurev.ea.18.050190.000415.

DeCelles, P.G., and Mitra, G., 1995, History of the Sevier orogenic wedge in terms of critical taper models, northeast Utah and southwest Wyoming: Geological Society of America Bulletin, v. 107, p. 454–462, https://doi.org/10.1130/0016-7606(1995)107<0454:HOTSOW>2.3.CO;2.

DeCelles, P.G., Carrapa, B., Gehrels, G.E., Chakraborty, T., and Ghosh, P., 2016, Along-strike continuity of structure, stratigraphy, and kinematic history in the Himalayan thrust belt: The view from northeastern India: Tectonics, v. 35, p. 2995–3027, https://doi.org/10.1002/2016TC004298.

Dettman, D.L., Fang, X., Garzione, C.N., and Li, J., 2003, Uplift-driven climate change at 12 Ma: A long $\delta^{18}O$ record from the NE margin of the Tibetan plateau: Earth and Planetary Science Letters, v. 214, p. 267–277, https://doi.org/10.1016/S0012-821X(03)00383-2.

Gavillot, Y., Meigs, A.J., Sousa, F.J., Stockli, D., Yule, D., and Malik, M., 2018, Late Cenozoic foreland-to-hinterland low-temperature exhumation history of the Kashmir Himalaya: Tectonics, v. 37, p. 3041–3068, https://doi.org/10.1029/2017TC004668.

Ghoshal, S., McQuarrie, N., Robinson, D.M., Adhikari, D.P., Morgan, L.E., and Ehlers, T.A., 2020, Constraining central Himalayan (Nepal) fault geometry through integrated thermochronology and thermokinematic modeling: Tectonics, v. 39, e2020TC006399, https://doi.org/10.1029/2020TC006399.

Hirschmiller, J., Grujic, D., Bookhagen, B., Coutand, I., Huyghu, P., Mugnier, J.-L., and Ojha, T., 2014, What controls the growth of the Himalayan foreland fold-and-thrust belt?: Geology, v. 42, p. 247–250, https://doi.org/10.1130/G35057.1.

Kellett, D.A., Cottle, J.M., and Larson, K.P., 2018, The South Tibetan Detachment System: History, advances, definition, and future directions, *in* Treloar, P.J., and Searle, M.P., eds., Himalayan Tectonics: A Modern Synthesis: Geological Society [London] Special Publication 483, p. 377–400, https://doi.org/10.1144/SP483.2.

Khanal, S., 2014, Structural and kinematic evolution of the Himalayan thrust belt, central Nepal [Ph.D. thesis]: Tuscaloosa, University of Alabama, 185 p.

Khanal, S., and Robinson, D.M., 2013, Upper crustal shortening and forward modeling of the Himalayan thrust belt along the Budhi-Gandaki River, central Nepal: International Journal of Earth Sciences, v. 102, p. 1871–1891, https://doi.org/10.1007/s00531-013-0889-1.

Kohn, M.J., 2008, *P-T-t* data from central Nepal support critical taper and repudiate large-scale channel flow of the Greater Himalayan Sequence: Geological Society of America Bulletin, v. 120, p. 259–273, https://doi.org/10.1130/B26252.1.

Kohn, M.J., Wieland, M.S., Parkinson, C.D., and Upreti, B.N., 2004, Miocene faulting at plate tectonic velocity in the central Himalaya, Nepal: Earth and Planetary Science Letters, v. 228, p. 299–310, https://doi.org/10.1016/j.epsl.2004.10.007.

Law, R.D., Searle, M.P., and Godin, L., eds., 2006, Channel Flow, Ductile Extrusion and Exhumation in Continental Collision Zones: Geological Society [London] Special Publication 268, 611 p.

Long, S., McQuarrie, N., Tobgay, T., and Grujic, D., 2011, Geometry and crustal shortening of the Himalayan fold-thrust belt, eastern and central Bhutan: Geological Society of America Bulletin, v. 123, p. 1427–1447, https://doi.org/10.1130/B30203.1.

Mandal, S., Robinson, D.M., Kohn, M.J., Khanal, S., and Das, O., 2019, Examining the tectono-stratigraphic architecture, structural geometry, and kinematic evolution of the Himalayan fold-thrust belt, Kumaun, northwest India: Lithosphere, v. 11, p. 414–435, https://doi.org/10.1130/L1050.1.

McQuarrie, N., Ehlers, T.A., Barnes, J.B., and Meade, B., 2008, Temporal variation in climate and tectonic coupling in the central Andes: Geology, v. 36, p. 999–1002, https://doi.org/10.1130/G25124A.1.

McQuarrie, N., Tobgay, T., Long, S.P., Reiners, P.W., and Cosca, M.A., 2014, Variable exhumation rates and variable displacement rates: Documenting recent slowing of Himalayan shortening in western Bhutan: Earth and Planetary Science Letters, v. 386, p. 161–174, https://doi.org/10.1016/j.epsl.2013.10.045.

McQuarrie, N., Eizenhöfer, P.R., Long, S.P., Tobgay, T., Ehlers, T.A., Reiners, P.W., Blythe, A.E., Morgan, L.E., Gilmore, M.E., and Dering, G.M., 2019, The influence of foreland structures on hinterland cooling: Evaluating the drivers of exhumation in the eastern Bhutan Himalaya: Tectonics, v. 38, p. 3282–3310, https://doi.org/10.1029/2018TC005340.

Parui, C., and Bhattacharyya, K., 2018, Duplex and along-strike structural variation: A case study from Sikkim Himalayan fold thrust belt: Journal of Structural Geology, v. 113, p. 62–75, https://doi.org/10.1016/j.jsg.2018.05.017.

Perrin, C., Clemenzi, L., Malavieille, J., Molli, G., Taboada, A., and Dominguez, S., 2013, Impact of erosion and décollements on large-scale faulting and folding in orogenic wedges: Analogue models and case studies: Journal of the Geological Society, v. 170, p. 893–904, https://doi.org/10.1144/jgs2013-012.

Robinson, D.M., and Martin, A.J., 2014, Reconstructing the Greater Indian margin: A balanced cross section in central Nepal focusing on the Lesser Himalayan duplex: Tectonics, v. 33, p. 2143–2168, https://doi.org/10.1002/2014TC003564.

Robinson, D.M., DeCelles, P.G., Garzione, C.N., Pearson, O.N., Harrison, T.M., and Catlos, E.J., 2003, Kinematic model of the Main Central thrust in Nepal: Geology, v. 31, p. 359–362, https://doi.org/10.1130/0091-7613(2003)031<0359:KMFTMC>2.0.CO;2.

Robinson, D.M., DeCelles, P.G., and Copeland, P., 2006, Tectonic evolution of the Himalayan thrust belt in western Nepal: Implications for channel flow models: Geological Society of America Bulletin, v. 118, p. 865–885, https://doi.org/10.1130/B25911.1.

Schelling, D., 1992, The tectonostratigraphy and structure of the eastern Nepal Himalaya: Tectonics, v. 11, p. 925–943, https://doi.org/10.1029/92TC00213.

Schelling, D., and Arita, K., 1991, Thrust tectonics, crustal shortening, and the structure of the far-eastern Nepal Himalaya: Tectonics, v. 10, p. 851–862, https://doi.org/10.1029/91TC01011.

Srivastava, P., and Mitra, G., 1994, Thrust geometries and deep structure of the outer and lesser Himalaya, Kumaon and Garwal (India): Implications for evolution of the Himalayan fold-and-thrust belt: Tectonics, v. 13, p. 89–109, https://doi.org/10.1029/93TC01130.

van Hinsbergen, D.J.J., Steinberger, B., Doubrovine, P.V., and Gassmöller, R., 2011, Acceleration and deceleration of India-Asia convergence since the Cretaceous: Roles of mantle plumes and continental collision: Journal of Geophysical Research, v. 116, B06101, https://doi.org/10.1029/2010JB008051.

Webb, A.A.G., 2013, Preliminary balanced palinspastic reconstruction of Cenozoic deformation across the Himachal Himalaya (northwestern India): Geosphere, v. 9, p. 572–587, https://doi.org/10.1130/GES00787.1.

Yin, A., 2006, Cenozoic tectonic evolution of the Himalayan orogen as constrained by along-strike variation of structural geometry, exhumation history, and foreland sedimentation: Earth-Science Reviews, v. 76, p. 1–131, https://doi.org/10.1016/j.earscirev.2005.05.004.

Printed in USA